

Multifunctional Nanoparticles Possessing A “Magnetic Motor Effect” for Drug or Gene Delivery**

Tae-Jong Yoon, Jun Sung Kim, Byung Geol Kim, Kyeong Nam Yu, Myung-Haing Cho,* and Jin-Kyu Lee*

Magnetic ferrite nanoparticles (usually called ferrofluid) have been widely used in various applications, such as smart seal magnetic circuits,^[1] audio speakers,^[2] and magnetic domain detectors.^[3] Recently, magnetic nanoparticles have been suggested for many new applications in high-density magnetic data storage,^[4] magnetic resonance imaging,^[5] catalyst supporters,^[6] and biomedical applications, such as magnetic carriers for bioseparation,^[7] enzyme and protein immobilization,^[8] and contrast-enhancing media.^[9] Transmission electron microscopy (TEM) or magnetic resonance imaging (MRI) have been used to observe magnetic nanoparticles incorporated within cells. However, TEM or MRI are not convenient for in situ monitoring, and thus a sensitive and easy technique for monitoring the nanoparticles in cells in situ is desirable. Confocal laser scanning microscopy (CLSM) is a highly sensitive detection technique specific to the fluorescence wavelength of the dye used. Incorporation of a fluorescent dye into the nanoparticle would enable the detection and monitoring, in situ, of the movement of the nanoparticles under an external magnetic field, for example.

Nanoparticles have been coated with a shell of stable and biocompatible material, such as silica (SiO₂), to avoid potential toxic effects on cells.^[10–12] Incorporation of a fluorescent dye into the silica shell seemed a good choice to

us. The polyvinylpyrrolidone (PVP) method has been applied to particles having ionic surface charges to generate a sol–gel silica coating with thickness which can be altered by varying the amount of tetraethoxysilane (TEOS) loaded.^[13] Herein, we report the preparation, employing a modified PVP method, of cobalt ferrite magnetic nanoparticles coated with a shell of amorphous silica, which contains luminescent organic dyes, such as rhodamine B isothiocyanate (RITC, orange, $\lambda_{\max(\text{em})} = 555 \text{ nm}$) or fluorescein isothiocyanate (FITC, green, $\lambda_{\max(\text{em})} = 518 \text{ nm}$) on the inside of the silica shell and biocompatible poly(ethylene glycol) (PEG) on the outside. We wished to determine whether the fluorescence characteristics of the organic dye could be used in conjunction with CLSM to compare the efficiency of uptake into cells of magnetic nanoparticles with and without PEG modification. Monitoring the movement of doped cells under an external magnetic field was also investigated because of its potential use in bioseparation and related applications.

Water-soluble bare cobalt ferrite magnetic nanoparticles of average size about 9 nm, synthesized by a slight modification of the co-precipitation method from FeCl₃·6H₂O and CoCl₂·6H₂O in hot basic NaOH solution,^[14] were stabilized with PVP to make them homogeneously dispersed in ethanol. The mixed solution of TEOS and dye-modified silane compound, synthesized from 3-aminopropyltriethoxysilane (APS) and dye-isothiocyanate,^[15] was polymerized on the surface of PVP-stabilized cobalt ferrites by adding ammonia solution as a catalyst to form organic-dye-incorporated cobalt ferrite–silica core–shell nanoparticles. The ratio of the concentrations of cobalt ferrite magnetic nanoparticles (Co ferrite MNPs) and TEOS was optimized to prevent the homogeneous nucleation of silica and to control the silica-shell thickness of the core–shell Co ferrite–silica MNPs. The TEM images in Figure 1 of silica-coated Co ferrite MNPs

[*] T.-J. Yoon,^[1] B. G. Kim, Prof. J.-K. Lee
Materials Chemistry Laboratory
School of Chemistry
Seoul National University
Seoul, 151-747 (Korea)
Fax: (+82) 2-882-1080
E-mail: jinklee@snu.ac.kr

J. S. Kim,^[2] K. N. Yu, Prof. M.-H. Cho
Laboratory of Toxicology
College of Veterinary Medicine and
School of Agricultural Biotechnology
Seoul National University
Seoul, 151-747 (Korea)
Fax: (+82) 2-873-1268
E-mail: mchotox@snu.ac.kr

[†] These authors contributed equally to this work.

[**] This work is supported by Nano Systems Institute-National Core Research Center (NSI-NCRC), Korea Science and Engineering Foundation (KOSEF). T.-J.Y., J.S.K., B.-G.K., and K.N.Y. are grateful for the award of a BK21 fellowship. We thank Prof. Seung Bum Park for his valuable comments and Ms. Eun Jung Kang for her help with CLSM investigations. “Magnetic motor effect”: cell movement as a result of applying an external magnetic field to cells containing magnetic nanoparticles.

Supporting information for this article is available on the WWW under <http://www.angewandte.org> or from the author.

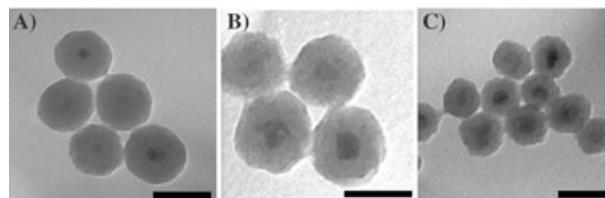


Figure 1. TEM images of Co ferrite–silica (core–shell) MNPs with controlled shell thicknesses. A) TEOS/MNP = 0.12 mg/4 mg, scale bar = 100 nm, B) TEOS/MNP = 0.06 mg/4 mg, scale bar = 50 nm, C) TEOS/MNP = 0.03 mg/4 mg, scale bar = 50 nm. As the ratio of TEOS/MNP (w/w) decreases, the shell thickness decreases.

prepared using different ratios of TEOS/MNP show that the thickness of the silica shell can be precisely controlled to produce core–shell nanoparticles with diameters ranging from 30 to 80 nm as the amount of TEOS was increased from 0.03 to 0.12 mg. The crystallinity and magnetic properties of the core material did not change upon coating with silica (see Supporting Information). PEG was easily attached to the silica-shell surface by adding PEG-Si(OMe)₃ solution after the shell formation was complete (see Supporting Information). This approach could be directly applied to the

synthesis of dye-labeled and surface-modified core-shell magnetic nanoparticles, $\text{MNP-SiO}_2(\text{RITC or FITC})$ and $\text{MNP-SiO}_2(\text{RITC or FITC})\text{-PEG}$. Attachment of PEG did not significantly change the size of the nanoparticles (determined by TEM measurements). The average diameter of the organic-dye-labeled Co ferrite-silica (core-shell) MNPs used in this study was about 50 nm as shown in Figure 1 B.

Although photobleaching is a common problem when fluorescent dyes are used, no significant photobleaching was observed in our rigid matrix system, as reported for a similar embedded system,^[16] and thus fluorescence intensity could be used to quantitatively analyze the quantity of core-shell nanoparticles incorporated into cells. The CLSM images in Figure 2 show breast cancer cells (MCF-7) after 24 h of

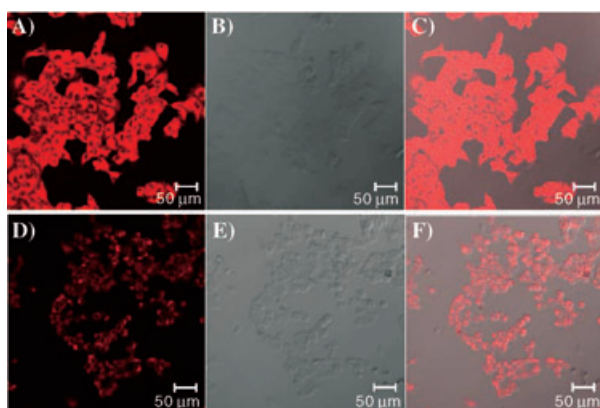


Figure 2. CLSM images of breast cancer cells after growth in media containing $\text{MNP-SiO}_2(\text{RITC})\text{-PEG}$ (A–C) or $\text{MNP-SiO}_2(\text{RITC})$ nanoparticles (D–F). (A and D: fluorescence images; B and E: bright-field images; C and F: overlay of the fluorescence and bright-field images).

growth in media containing $\text{MNP-SiO}_2(\text{RITC})\text{-PEG}$ (PEG-modified nanoparticle, Figure 2 A–C) and $\text{MNP-SiO}_2(\text{RITC})$ (unmodified, Figure 2 D–F). From the overlay images (Figure 2 C and F) of the fluorescence images (Figure 2 A and D) and bright-field images (Figure 2 B and E), respectively for both samples, it seems that the surface modification by PEG enhances the incorporation of Co ferrite MNP into cells. Thus all subsequent experiments were conducted using $\text{MNP-SiO}_2(\text{RITC})\text{-PEG}$.

If dyes having different fluorescence emission wavelengths are used, the position of the nanoparticles containing different dyes could be selectively monitored simultaneously at the respective emission wavelength. The CLSM images in Figure 3 show breast cancer cells (MCF-7) containing $\text{MNP-SiO}_2(\text{RITC})\text{-PEG}$ or $\text{MNP-SiO}_2(\text{FITC})\text{-PEG}$ clearly emitting at different wavelengths, with orange light from RITC and green light from FITC. By changing the focus distances, CLSM could “slice” the cell images at different z positions to clearly show that emission did not emerge from the organic-dye-labeled core-shell MNPs adsorbed on the cell membrane surface, but from what was delivered into the cytoplasm of living cells. It was also confirmed that core-shell MNPs could not penetrate the nucleus as there was no emission from the nucleus (Figure 3 B and E).

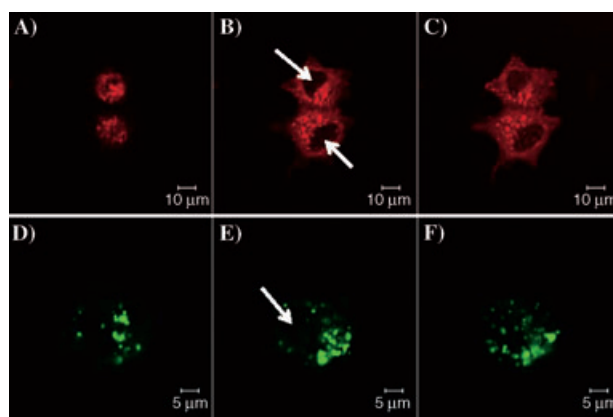


Figure 3. CLSM z-sectioned images of breast cancer cells obtained by using $\text{MNP-SiO}_2(\text{RITC})\text{-PEG}$ (A–C) and $\text{MNP-SiO}_2(\text{FITC})\text{-PEG}$ (D–F). (A and D: top slices; B and E: middle slices; C and F: bottom slices). The white arrows indicate the position of nucleus.

For the time-dependent studies of the uptake of $\text{MNP-SiO}_2(\text{RITC})\text{-PEG}$ nanoparticles by live MCF-7 cells, the cells were attached to a glass cover slip, a culture solution containing $\text{MNP-SiO}_2(\text{RITC})\text{-PEG}$ nanoparticles was loaded onto the cover slip and CLSM fluorescence images were taken every 5 minutes (Figure 4). As time elapsed, the

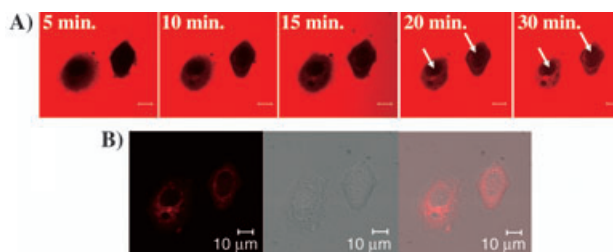


Figure 4. MCF-7 cells mixed with a culture of $\text{MNP-SiO}_2(\text{RITC})\text{-PEG}$ solution. Cells were recorded for 30 min with a video camera and up to 48 h by time-elapse photography. A) Representative pictures captured at 5 min intervals. As time elapsed, we could clearly determine the location of the nucleus (white arrow). B) After saturation with $\text{MNP-SiO}_2(\text{RITC})\text{-PEG}$, the media was removed and the cell sample carefully washed. The CLSM measurements show fluorescent emissions only from the internalized $\text{MNP-SiO}_2(\text{RITC})\text{-PEG}$ nanoparticles. (left: fluorescence image; middle: bright-field image; right: merged image).

dark cytoplasm region in the cell faded and turned into an orange emissive region owing to the uptake of $\text{MNP-SiO}_2(\text{RITC})\text{-PEG}$, and the position of the nucleus became clearly visible (Figure 4 A). The cell was saturated with dye-labeled core-shell nanoparticle within 30 min, and no significant intensity difference in the cytoplasm area nor emission from the nucleus region were detected during the next 48 h. After saturation, the culture solution containing the excess of $\text{MNP-SiO}_2(\text{RITC})\text{-PEG}$ nanoparticles was removed and the sample carefully washed with a new culture solution (that did not contain $\text{MNP-SiO}_2(\text{RITC})\text{-PEG}$ nanoparticles). Subsequent CLSM measurement of the sample showed that the fluorescent emissions came from the internalized MNP-

SiO₂(RITC)-PEG nanoparticles (Figure 4B); all the emission from the culture solution containing MNP-SiO₂(RITC)-PEG nanoparticles around the cells was removed. The internalization process seems to follow the mechanism of normal endocytosis, which allows the internalization of core-shell MNPs into various cells including mammalian lung normal cells (NL-20), lung cancer cells (A-549), and breast cancer cells (MCF-7). After they had been subjected to 24 h starvation, MCF-7, NL-20, and A-549 cells were treated with MNP-SiO₂(RITC or FITC)-PEG, and the cell viability was measured by a 3-(4,5-dimethylthiazol-2-yl)-2,5-diphenyltetrazolium bromide (MTT) assay. In this condition, the cell viability was maintained at greater than 90% in all groups indicating that the Co ferrite-silica core-shell MNPs, MNP-SiO₂(RITC or FITC)-PEG, do not show acute cytotoxicity at the level of a few tenths of a microgram (80 μg mL⁻¹) within 48 h.

Once we were convinced by fluorescence experiments and inductively coupled plasma atomic emission spectrometry (ICP-AES) measurements that a considerable quantity of the MNPs were incorporated into cells (uptake about 10⁵ nanoparticles per cell), we attempted to monitor the movement of cells containing MNPs under an external magnetic field (Figure 5)—this movement is anticipated to be an advantageous property of MNPs for real biological applications, such as cell separation and drug- or gene-delivery carrier.

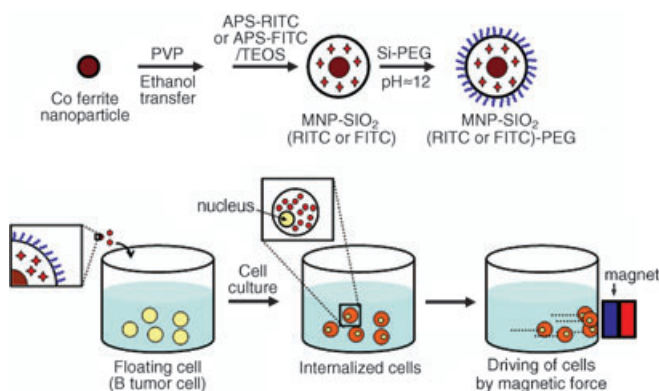


Figure 5. Schematic illustration of the overall synthetic procedure for MNP-SiO₂(RITC)-PEG and the movement of cells containing magnetic nanoparticles by an external magnetic force.

Microscope images in Figure 6 were captured every 0.2 s from the video camera focused in the area near the container wall (about 1 cm away) while an external magnetic field was applied with a commercial Nd-Fe-B magnet (≈ 0.3 Tesla) on the outside of the Petri dish (upper-left position in Figure 6), containing floating B tumor cells internalized with MNP-SiO₂(RITC)-PEG nanoparticles. As observed in the captured microscope images of Figure 6, B tumor cells that had sunk to the bottom of the Petri dish moved relatively slowly at a speed of approximately 0.2 mm s⁻¹, probably owing to interaction with the bottom surface. However, floating cells moved very fast at a speed of approximately 1.0 mm s⁻¹. When the external magnet was removed and reapplied to the outside of Petri dish, the movement of cells was halted and restarted

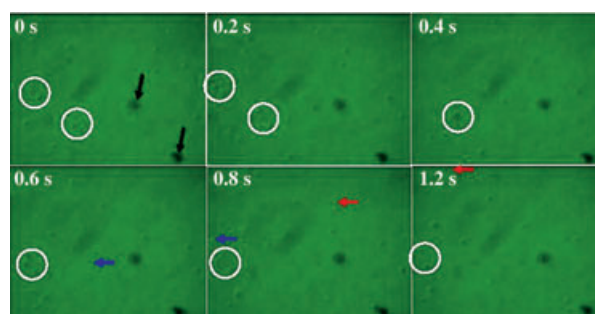


Figure 6. Optical microscope images of floating B tumor cells. Images were captured every 0.2 seconds (see video in Supporting Information). The external magnetic field direction is towards the upper-left corner, and B tumor cells that had sunk to the bottom of the dish moved relatively slowly to that direction (white circles), while floating B tumor cells moved much faster (blue and red arrows). The black arrows denote the standard direction of cell movements at the bottom surface of the dish.

again. Moving the position of external magnet could also easily change the direction of the cell movement. To our knowledge, this is the first clear observation of the “magnetic motor effect”: cell movement as a result of applying an external magnetic field to cells containing magnetic nanoparticles. Surprisingly, the speed of the cell movement is quite fast, confirming that the amount of internalized MNPs in our system was sufficiently high to show a magnetic motor effect while not causing any cytotoxicity.

In summary, the organic-dye-labeled Co ferrite-silica (core-shell) magnetic nanoparticles have been prepared by a modified polyvinylpyrrolidone (PVP) method and the sol-gel process. The thickness of the silica shell could be easily controlled by adjusting the ratio of magnetic nanoparticle to tetraethoxysilane (TEOS) and dye-modified silane. Core-shell magnetic nanoparticles could also be labeled with two different organic dyes, such as rhodamine B isothiocyanate (RITC) and fluorescent isothiocyanate (FITC), and the nanoparticle surface could be modified with bio-inert poly(ethylene glycol) (PEG) groups, providing multifunctional magnetic and optical properties along with biocompatibility. We investigated the internalization efficiencies of MNP-SiO₂(RITC or FITC), and MNP-SiO₂(RITC or FITC)-PEG in various in vitro cell studies and clearly observed the external magnetic motor effect on floating cells internalized with MNPs. These basic results on core-shell MNPs are expected to lead to applications in cell separation, biological labeling and detection, and drug and gene delivery.

Experimental Section

FeCl₃·6H₂O, CoCl₂·6H₂O, and Fe(NO₃)₃·9H₂O (Sigma-Aldrich), RITC and FITC organic dyes (Fluka), APS, TEOS, and PEG-Si(OMe)₃ (Gelest) were used without further purification.

MNP-SiO₂(RITC or FITC)-PEG: Cobalt ferrite solution (34.7 mL, 20 mg MNP mL⁻¹ solution in water) was added to polyvinylpyrrolidone solution (PVP; 0.65 mL; *M*, 55,000 Da, 25.6 g L⁻¹ in H₂O), and the mixture was stirred for 1 day at room temperature. The PVP-stabilized cobalt ferrite nanoparticles were separated by addition of aqueous acetone (H₂O/acetone = 1/10, v/v) and centrifugation at 4000 rpm for 10 min. The supernatant solution was removed, and

the precipitated particles were redispersed in ethanol (10 mL). Multigram-scale preparation of PVP-stabilized cobalt ferrite nanoparticles was easily reproduced in this modified synthetic method. Trimethoxysilane modified by rhodamine B isothiocyanate (RITC) was prepared from 3-aminopropyltriethoxysilane (APS) and rhodamine B isothiocyanate under nitrogen using a standard Schlenk line technique.^[10,15] A mixed solution of TEOS and RITC-modified trimethoxysilane (TEOS/RITC-silane molar ratio = 0.3/0.04) was injected into the ethanol solution of PVP-stabilized cobalt ferrite. Polymerization initiated by adding ammonia solution (0.86 mL; 30 wt% by NH₃) as a catalyst produced cobalt ferrite–silica core–shell nanoparticles containing organic dye. These nanoparticles were dispersed in ethanol and precipitated by ultra-centrifugation (18000 rpm, 30 min). The purified core–shell nanoparticles (45 mg) were redispersed in absolute ethanol (10 mL) and then treated with 2-[methoxy(polyethyleneoxy)propyl]trimethoxy-silane (PEG-Si(OMe)₃; 125 mg, 0.02 mmol), CH₃O(CH₂CH₂O)₆₋₉CH₂CH₂CH₂Si(OCH₃)₃, at pH ≈ 12 (adjusted with NH₄OH). The resulting MNP-SiO₂(RITC)-PEG was washed and centrifuged in EtOH several times and characterized by IR spectroscopy (C–H stretching band at 2800–2900 cm⁻¹). MNP-SiO₂(FITC)-PEG could also be prepared by a similar method by using FITC-silane instead of RITC-silane. All the prepared nanoparticles were characterized by TEM, FT-IR, UV/Vis absorption and emission spectroscopy, and vibrating sample magnetometer (VSM) measurements.

Cell culture: Breast cancer cells (mammary gland adenocarcinoma, MCF-7), normal human bronchial epithelial cells (NL-20), and lung cancer cells (A-549) were from American Type Culture Collection. MCF-7 cells were grown in DMEM (Cambrex Bio Science) containing 10% FBS (v/v) and MNP-SiO₂(RITC or FITC)-PEG (40 μL, 2 mg mL⁻¹). NL-20 and A-549 were grown in RPMI (Cambrex Bio Science) under the same conditions. All cells were cultured in Lab-Tek glass chamber slides (Nalge Nunc International) to facilitate fluorescence emission by confocal laser scanning microscopy (CLSM).

MTT assay: The cells were incubated in a 96-well plate. At the end of the incubation period, 3-(4,5-dimethylthiazol-2-yl)-2,5-diphenyltetrazolium bromide (MTT; 50 μL, Sigma-Aldrich) in pH = 7.2 phosphate buffered saline (PBS; 0.2 mg mL⁻¹) was added to each well (final concentration of 0.4 mg mL⁻¹) and cultures were incubated in 5% CO₂ for 4 h at 37°C. Then the culture medium was carefully removed by pipetting, and the formazan crystals generated by dehydronase activity in mitochondria, which only occurs in living cells, were dissolved in DMSO (150 μL) for analysis. After 10 min agitation on a shaker, absorbance was measured at 490 nm and 620 nm for test and reference solutions, respectively.

CLSM: 3D image reconstructions of organic-dye-labeled nanoparticles were obtained with a Zeiss LSM 510 CLSM equipped with a computer-controlled scan stage. An argon laser for RITC excitation at 543 nm (488 nm for FITC) was used for imaging. For each cell, more than 10 optical planes were scanned by changing the focal length to detect the nanoparticles at different locations within the cell. In experiments involving live cells, an exclusive culture chamber was used to maintain a cell culture temperature of 37°C.

Determination of the quantity of nanoparticles in cells: The total number of cells in the magnetic motor experiment (Figure 6) was estimated to be 4.0 × 10⁵ by using a hemacytometer chamber. ICP-AES measurement, after the cells containing nanoparticles were destroyed and nanoparticles were completely dissolved with concentrated HCl, reveals the quantity of cobalt ion in each cell to be approximately 10⁻¹³ mmol. From calculation, each 9-nm CoFe₂O₄ nanoparticle contains about 10⁻¹⁸ mmol of Co ions. Therefore, the number of magnetic nanoparticles in each cell in our magnetic motor effect experiments can be estimated to be of the order of 10⁵.

Received: September 7, 2004

Published online: January 5, 2005

Keywords: bioinorganic chemistry · fluorescent probes · hybrid materials · magnetic properties · nanotechnology

- [1] K. Furumura, H. Sugi, Y. Murakami, H. Asai, US patent 4598914, **1986**.
- [2] J. A. King, US patent 4,017,694, **1977**.
- [3] a) D. H. Han, H. L. Luo, Z. Yang, *J. Magn. Magn. Mater.* **1996**, *161*, 376–378; b) H. Fujiwara, *J. Appl. Phys.* **1993**, *73*, 5757–5762.
- [4] a) Q. Song, Z. J. Zhang, *J. Am. Chem. Soc.* **2004**, *126*, 6164–6168; b) H. Zeng, J. Li, J. P. Liu, Z. L. Wang, S. Sun, *Nature* **2002**, *420*, 395–398; c) C. Liu, B. Zou, A. J. Rondinone, Z. J. Zhang, *J. Am. Chem. Soc.* **2000**, *122*, 6263–6267.
- [5] a) J. M. Perez, L. Josephson, T. O’Loughlin, D. Högemann, R. Weissleder, *Nat. Biotechnol.* **2002**, *20*, 816–820; b) J. M. Perez, T. O’Loughlin, F. J. Simeone, R. Weissleber, L. Josephson, *J. Am. Chem. Soc.* **2002**, *124*, 2856–2857; c) L. Babes, B. Denizot, G. Tanguy, J. J. L. Jeune, P. Jallet, *J. Colloid Interface Sci.* **1999**, *212*, 474–482.
- [6] T. J. Yoon, W. Lee, Y. S. Oh, J. K. Lee, *New J. Chem.* **2003**, *27*, 227–229.
- [7] a) P. S. Doyle, J. Bibette, A. Bancaud, J. Viovy, *Science* **2002**, *295*, 2237; b) H. Gu, P. Ho, K. W. T. Tsang, L. Wang, B. Xu, *J. Am. Chem. Soc.* **2003**, *125*, 15702–15703; c) D. Wang, J. He, N. Rosenzweig, Z. Rosenzweig, *Nano Lett.* **2004**, *4*, 409–413.
- [8] a) D. Cao, P. He, N. Hu, *Analyst* **2003**, *128*, 1268–1274; b) T. Mirzabekov, H. Kontos, M. Farzan, W. Marasco, J. Sodroski, *Nat. Biotechnol.* **2000**, *18*, 649–654; c) J. P. Chen, W. S. Lin, *Enzyme Microb. Technol.* **2003**, *32*, 801–811; d) K. Nishimura, M. Hasegawa, Y. Ogura, T. Nishi, K. Kataoka, H. Handa, M. Abe, *J. Appl. Phys.* **2002**, *91*, 8555–8556; e) I. Willner, E. Katz, *Angew. Chem. Int. Ed.* **2003**, *42*, 4576–4588.
- [9] E. X. Wu, H. Tang, K. K. Wong, J. Wang, *J. Magn. Reson. Imaging* **2004**, *19*, 50–58; b) J. M. Perez, L. Josephson, R. Weissleder, *ChemBioChem* **2004**, *5*, 261–264.
- [10] Y. Lu, Y. Yin, B. T. Mayers, Y. Xia, *Nano Lett.* **2002**, *2*, 183–186.
- [11] M. A. Correa-Duarte, M. Giersig, N. A. Kotov, L. M. Liz-Marzán, *Langmuir* **1998**, *14*, 6430–6435.
- [12] a) A. Kros, M. Gerritsen, V. S. I. Sprakel, N. A. J. M. Sommerdijk, J. A. Jansen, R. J. M. Nolte, *Sens. Actuators B* **2001**, *81*, 68–75; b) Y. Shchipunov, *J. Colloid Interface Sci.* **2003**, *268*, 68–76.
- [13] a) C. Graf, D. L. J. Vossen, A. Imhof, A. van Blaaderen, *Langmuir* **2003**, *19*, 6693–6700.
- [14] a) D. Zins, V. Cabuil, R. Massart, *J. Mol. Liq.* **1999**, *83*, 217–232; b) M. H. Sousa, F. A. Tourinho, J. Depeyrot, G. J. da Silva, M. C. F. L. Lara, *J. Phys. Chem. B* **2001**, *105*, 1168–1175.
- [15] a) N. A. M. Verhaegh, A. van Blaaderen, *Langmuir* **1994**, *10*, 1427–1438; b) A. van Blaaderen, V. Vrij, *Langmuir* **1992**, *8*, 2921–2931.
- [16] a) S. Santra, P. Zhang, K. Wang, R. Tapeç, W. Tan, *Anal. Chem.* **2001**, *73*, 4988–4993; b) K. P. McNamara, Z. Rosenzweig, *Anal. Chem.* **1998**, *70*, 4853–4859.